

Dynamic analysis and QFT-based robust control design of a coaxial micro-helicopter

Aissa Meksi, Ahmed HamidaBoudinar, BenatmanKouadri

Electrical Engineering Department, Faculty of Electrical Engineering,
University of Sciences and Technology of Oran, Algeria

Article Info

Article history:

Received Mar 9, 2019

Revised Apr 19, 2019

Accepted Apr 25, 2019

Keywords:

Coaxial micro-helicopter

MATLAB toolbock

Non-linear

Quantitative feedbacktheory

ABSTRACT

This paper presents the dynamic behavior of a coaxial micro-helicopter, under Quantitative Feedback Theory (QFT) control. The flight dynamics of autonomous air vehicles (AAVs) with rotating rings is non-linear and complex. Then, it becomes necessary to characterize these non-linearities for each flight configuration, in order to provide these autonomous air vehicles (AAVs) with autonomous flight and navigation capabilities. Then, the nonlinear model is linearized around the operating point using some assumptions. Finally, a robust QFT control law over the coaxial micro-helicopter is applied to meet some specifications. QFT (quantitative feedback theory) is a control law design method that uses frequency domain concepts to meet performance specifications while managing uncertainty. This method is based on the feedback control when the plant is uncertain or when uncertain disturbances are affecting the plant. The QFT design approach involves conventional frequency response loop shaping by manipulating the gain variable with the poles and zeros of the nominal transfer function. The design process is accomplished by using MATLAB environment software.

*Copyright © 2019 Institute of Advanced Engineering and Science.
All rights reserved.*

Corresponding Author:

Aissa Meksi,

Electrical Engineering Department, Faculty of Electrical Engineering,

University of Sciences and Technology of Oran,

B.P 1505, El Mnaouer, Oran, Algeria.

Email: aissa.meksi@univ-usto.dz

1. INTRODUCTION

Unmanned aerial vehicles (UAVs) are aircraft capable of flying and performing a mission without human presence on board. Initially developed as part of military activities, there is now a great potential for civil activities (surveillance, cartography...). Many unresolved constraints remain for the use of civil drones in the public space. Among the hard points to resolve are embedded decision-making autonomy, all-weather perception capability, safety and dependability. These features will, in the future, be subject to a certification process being developed, but current drones suffer from a lack of robustness and autonomy.

In the literature, modeling and development of new formulations of coaxial micro-helicopters have been the subject of several research works such as: Mohammad Harun works [1], and Chen [2] on classic helicopters, Alvaro [3] for the minidrone with a keeled propeller, as well as the works of Schafroth and Christian [4] on coaxial micro-helicopter (with fixed and variable steps).

Among these military drones a micro coaxial helicopter presented in this article was developed by partners ISL, CRAN and HEUDIASYC Systems. The more detailed models of some configurations of the coaxial micro-helicopter can be found in [5,6]. The coaxial micro-helicopter with swashplate consists of two counter-rotating rotors ensuring the lift and propulsion of the aircraft and a swashplate mounted at the lower rotor to control the craft. The two counter-rotating rotors share the same axis of rotation, which makes it possible to compensate mutually for the reaction torque produced by each of the rotors, and consequently the

steering of the lace. This system is also a compact anti-torque solution, which saves the auxiliary system present on a conventional helicopter and therefore reduce the length of the fuselage. The mass of the drone is lifted by the total thrust produced by the two rotors. A rotary wing drone can be considered as a rigid body with six degrees of freedom for which the aerodynamic forces generated by its actuators are added [7].

The problem of this coaxial micro-helicopter is non-linear, complex, quasi stationnaire and subject to wind disturbance, affecting its stable flight and easy landing and the dynamic equations of motion for a coaxial micro-helicopter including structured and unstructured uncertainties. The application of the QFT technique for trajectory tracking in the presence of uncertainties of mass variation parameters is studied. In this paper, the QFT Horowitz I.M method as an appropriate robust control method is applied to a coaxial micro-helicopter, which has many advantages over other relevant techniques [8].

The QFT Horowitz I.M design procedure is not only based on the amplitude of the transfer function in the frequency domain, but also takes into account the phase information [8]. The quantitative feedback theory QFT, called (La théorie quantitative de la retroaction TQR) in French Horowitz I.M, was developed by Isaac Horowitz. It is a frequency technique using the Nichols diagram to realize a robust control [9]. The desired temporal responses are translated into tolerances in the frequency domain. The design process is highly transparent; allowing a designer to see what tradeoff is needed to achieve a desired level of performance.

In this manuscript, we address the three main problems of the automatic applied to the coaxial helicopter micro-type drone, since we are interested in determining a dynamic model of the system, and aeronautical model, as well as calculating a stabilizing input. We are more specifically interested in achieving the objectives thus defined:

- Modeling the translation and rotation dynamics of the coaxial micro-helicopter during its autonomous flight phase[10].
- Establish the linear model of the nonlinear model by applying the Taylor approximation method around the operating point.
- Determine a stabilizing corrector for coaxial micro-helicopter in the case of quasi-stationary flight, from a sufficiently simple synthesis model[11].

The remainder of this paper is organized as follow. In Section2, the dynamic model of coaxial micro-helicopter is formulated in the Cartesian space. In Section3, QFT controller is developed and applied to the direct dynamic model of drone in Cartesian space. Section4 presents simulation results of the proposed controller and discussion of results. Finally, some conclusions are presented in the closing section.

2. MATHEMATICAL MODEL OF COAXIAL MICRO-HELICOPTER

Knowing that coaxial micro-helicopter is considered as a rigid body with fixed mass "m", the generic model with six degrees of freedom (6-DOF) refers to its three translations and its three spatial rotations. It therefore describes the dynamics and the kinematics of rotation and translation in the reference system linked to the "G" body. There are two ways of expressing the equations of motion: either from the laws of Newton and Euler that we will use or by reformulating the Newtonian mechanics with the Lagrange and Hamilton equations. In this section are defined the reference points, axes systems used and the kinematic and kinetic parameters appearing in Figure 1, as well as all the relations composing the 6-DOF model. It is assumed that the inertial effects of the rotors are negligible compared to those of the main body.

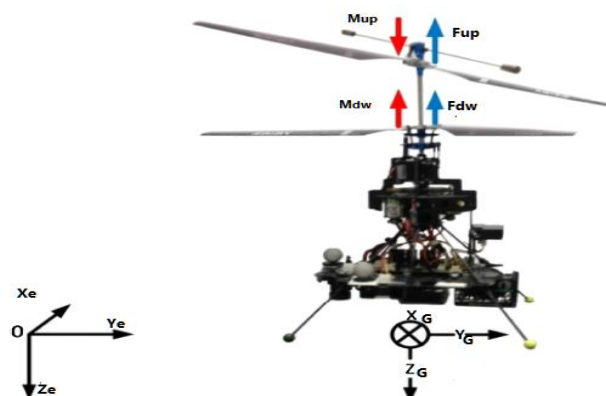


Figure 1. Landmarks used to describe the movement of the coaxial micro-helicopter

2.1. Reference and axes systems

The movement of a rigid body is mainly described by two references:

- The inertial reference $\{J\}$: bound to the Earth, having a reference point "O" and defined by the base $\{x_e; y_e; z_e\}$, where $\{x_e\}$ points north, $\{y_e\}$ points east, and $\{z_e\}$ points up.
- The navigation mark (gear or mobile) $\{B\}$: related to the center of gravity "G" of the structure of the drone and defined by the base $\{x_G; y_G; z_G\}$ where $\{x_G\}$ is the longitudinal axis pointing towards the vehicle front, $\{y_G\}$ defines the lateral axis and points to the vehicle right and $\{z_G\}$ defines the vertical axis of the vehicle and points to the top.

A rotation matrix identifies the orientation of any coordinate system in the three dimensions of space. It is also called transition matrix or attitude matrix, noted "R η ". Consequently, the passage matrix R η of the reference apparatus "B" to the reference inertial "J" is parameterized by the Euler angles describing the three rotation angles ϕ (roll), θ (pitch) and ψ (yaw). The product of these three matrices makes it possible to express the passage from the reference "B" to the reference "J", that is to say [12]:

$$R_\eta = \begin{bmatrix} \cos\theta\cos\psi & \sin\phi\sin\theta\cos\psi - \cos\phi\sin\psi & \cos\phi\sin\theta\cos\psi + \sin\phi\sin\psi \\ \cos\theta\sin\psi & \sin\phi\sin\theta\sin\psi + \cos\phi\cos\psi & \cos\phi\sin\theta\sin\psi - \sin\phi\cos\psi \\ -\sin\theta & \sin\phi\cos\theta & \cos\phi\cos\theta \end{bmatrix} \quad (1)$$

where ϕ is the roll angle, θ the pitch angle and ψ the yaw angle, respectively. The kinematic equation of orientation connects the time derivative of the angles of roll ϕ , pitch θ and yaw ψ to the instantaneous speed of rotation by:

$$Q_\eta = \begin{bmatrix} 1 & \tan\theta\sin\phi & \tan\theta\cos\phi \\ 0 & \cos\phi & -\sin\phi \\ 0 & \frac{\sin\phi}{\cos\theta} & \frac{\cos\phi}{\cos\theta} \end{bmatrix} \quad (2)$$

2.2. Balance of forces and moments applied

Equations of forces and moments are required to complete the dynamic modeling of aeromechanical systems. Moreover, the modeling of these forces and moments (that is to say, F_{res} and M_p) remains a major problem, due to the complexity of fluid dynamics and interactions between the studied vehicle (rigid body equipped with moving actuators) and the surrounding fluid. The main forces acting on a rotorcraft are presented [12].

2.2.1. Effort settings

The effort parameters are simply the three forces and the three moments that intervene in the dynamics of translation and rotation of the vehicle. The development of these efforts will constitute the aerodynamic model presented in the following sections [7, 12]. We note then:

$$F_{res} = [F_x F_y F_z]^T, \text{ the three components of the force vector expressed in "B",}$$

$$M_p = [M_x M_y M_z]^T, \text{ the three components of the moment vector expressed in "B".}$$

and

$$F = [F_x \quad F_y \quad F_z \quad M_x \quad M_y \quad M_z]^T \quad (3)$$

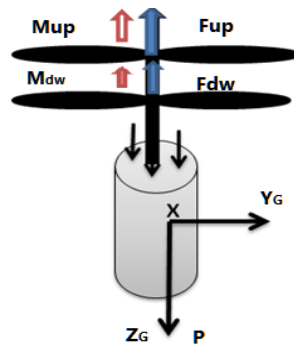


Figure 2. The forces and moments on the system

2.2.1.1. The forces

The forces which are acting on the system are:

- The weight of the coaxial micro-helicopter

The vehicle is subjected to the gravitational field as all bodies in the vicinity of the Earth, and the acceleration of gravity is denoted "g". The weight component "P" is the force to which the craft is subjected, and whose direction is normal to the surface of the Earth. The value of "g" is expressed and known in the inertial reference frame "B", that is to say [12]:

$$P = mgz_e \tag{4}$$

- The pushing force

The model of thrust of a rotary wing can be expressed as a function of the speed of rotation of the rotor squared Ω_p^2 at a certain aerodynamic coefficient "k". The lift generated by a rotating rotor therefore has the following expression:

$$F_p = k\Omega_p^2 \tag{5}$$

- The drag force

The aerodynamic drag force of the vehicle F_a caused by the friction of the air on the fuselage can be expressed as: [13]

$$F_a = k_{1d}\Omega^2 \tag{6}$$

Ω : Motor rotation speed.

2.2.2. Forces generated by the coaxial micro-helicopter

Thrust is the main force produced by the coaxial micro-helicopter, allowing the drone to move in three-dimensional space. The immobile upper rotor produces only a vertical thrust force F_1 , which is directly proportional to the square of the speed of rotation of its blades Ω_1 and the aerodynamic coefficient of thrust k_α , such that:

$$F_1 = [0 \quad 0 \quad k_\alpha\Omega_1^2]^T \tag{7}$$

The expression of the force F_2 generated by the lower rotor depends on the two angles δ_{cx} and δ_{cy} of the swashplate which form the inputs of the system. This force is given by:

$$F_2 = k_B\Omega_2^2 \begin{bmatrix} -\sin\delta_{cy}\cos\delta_{cx} \\ -\sin\delta_{cx} \\ \cos\delta_{cx}\cos\delta_{cy} \end{bmatrix} \tag{8}$$

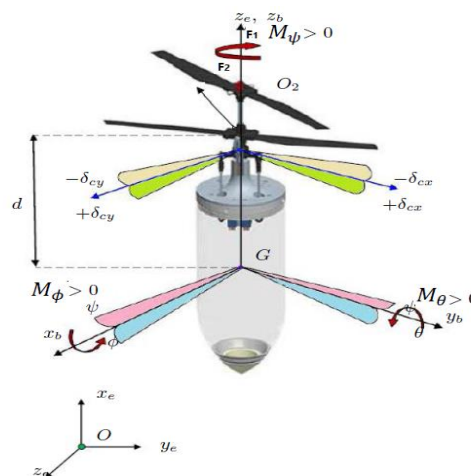


Figure 3. Summary of the elements related to the modeling of the coaxial micro-helicopter

The total thrust, $F = [0 \ 0 \ F_z]^T$, is defined by the sum of the individual thrusts of each of the rotors $[F_1]_{Zb}$ and $[F_2]_{Zb}$ described by (5) and (6). The expression of the total thrust can be written:

$$F_z = [k_a \Omega_1^2 + k_B \cos \delta_{cx} \cos \delta_{cy} \Omega_2^2] \quad (9)$$

Finally, the total force F generated by the two rotors can be written:

$$F_{res} = \begin{bmatrix} F_x \\ F_y \\ F_z \end{bmatrix} = \begin{bmatrix} -k_B \sin \delta_{cy} \cos \delta_{cx} \Omega_2^2 \\ -k_B \sin \delta_{cx} \Omega_2^2 \\ k_a \Omega_1^2 + k_B \cos \delta_{cx} \cos \delta_{cy} \Omega_2^2 \end{bmatrix} \quad (10)$$

2.2.3. Moments acting on the coaxial micro-helicopter

The moment M_p generated by the total force F applied to the coaxial micro-helicopter at its center of gravity G is therefore the sum of the moments resulting from the force of the upper rotor F_1 , that of the lower rotor F_2 and the weight P.

$$M_p = \overrightarrow{GO}_1 \wedge F_1 + \overrightarrow{GO}_2 \wedge F_2 + \overrightarrow{GG} \wedge P \quad (11)$$

As a conclusion, the sum of the moments of the forces F is given by:

$$M_p = \begin{bmatrix} -dk_B \sin \delta_{cx} \Omega_2^2 \\ dk_B \cos \delta_{cx} \sin \delta_{cy} \\ 0 \end{bmatrix} \quad (12)$$

However, a moment around the z axis due to each of the rotors is directly proportional to the square of their velocity with the aerodynamic coefficients $\gamma_1 > 0, \gamma_2 > 0$, such as:

$$M_\psi = [0 \ 0 \ \gamma_1 \Omega_1^2 - \gamma_2 \Omega_2^2]^T \quad (13)$$

Finally, the total moment M_p is given by:

$$M_p = \begin{bmatrix} M_\phi \\ M_\theta \\ M_\psi \end{bmatrix} = \begin{bmatrix} -dk_B \sin \delta_{cx} \Omega_2^2 \\ dk_B \cos \delta_{cx} \sin \delta_{cy} \Omega_2^2 \\ \gamma_1 \Omega_1^2 - \gamma_2 \Omega_2^2 \end{bmatrix} \quad (14)$$

According to (2.10) and (2.14), the expression of the total force F can be written as:

$$F = (0, 0, F_z)^T + \sum M_p \text{ where } \sum = \frac{1}{d} sk(z_e) \quad (15)$$

2.2.4. Development of the mathematical model according to Newton-Euler

After presenting the different equations we can now develop the model mathematical using the Newton-Euler formulation. The corresponding equations are written in the following form [7,12]:

$$\begin{aligned} \dot{\xi} &= v \\ m\dot{v} &= R_\eta T + P + F_{ext} \\ \dot{\eta} &= Q_\eta \Omega \\ J\dot{\Omega} &= -\Omega \times J\Omega + \tau + M_{ext} \end{aligned} \quad (16)$$

where:

ξ : Is the position vector of the coaxial micro-helicopter $\xi = [x, y, z]^T$,

m: the total mass of the coaxial micro-helicopter,

J: symmetric matrix inertia of dimension (3x3), given by:

$$J = \begin{bmatrix} I_x & 0 & 0 \\ 0 & I_y & 0 \\ 0 & 0 & I_z \end{bmatrix}, \quad (17)$$

Ω : The angular velocity expressed in the fixed inertial reference.

2.2.5. Dynamic simulation of the system in MATLAB-Simulink environment

MATLAB Simulink software is used to simulate the propulsion system. In Figure 4, as it is mentioned, a section of body modeling, called rigid body, is shown in Simulink environment. In this system, inputs, forces and the total drag force are exerted on the center of mass of the vehicle. Total drag forces, before entering the body dynamic calculations system, which are written based on Newton Euler’s law, are transferred from body coordinate system to inertia coordinate system. In this system, propulsion system and the transition of forces and moments from body coordinate system to inertia coordinate system are added to the rigid body sub-system. The physical properties of the coaxial micro-helicopter are considered as in Table 1.

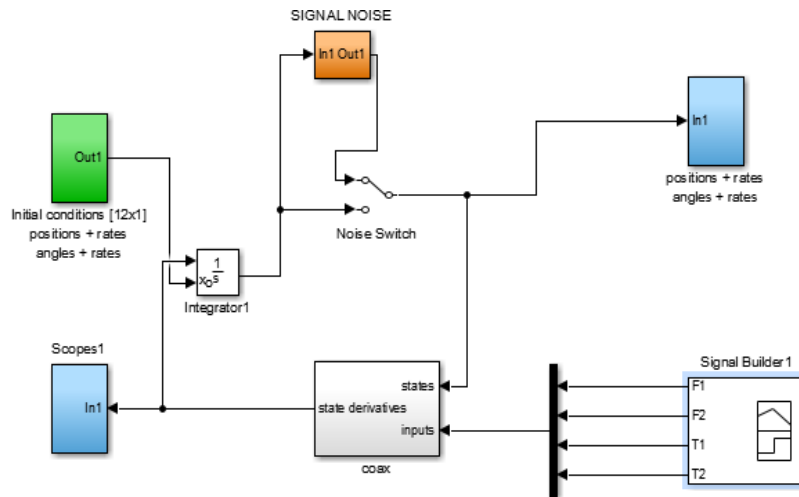


Figure 4. Nonlinear system of the coaxial micro-helicopter

Table 1. Parameters model of coaxial micro-helicopter

Parameter	Description	Value	Unit
m	mass(kg)	0.290	Kg
I_x	Moment of inertia about X axis	1.383×10^{-3}	kgm^2
I_y	Moment of inertia about Y axis	1.383×10^{-3}	kgm^2
I_z	Moment of inertia about Z axis	2.72×10^{-4}	kgm^2
d	Distance center of gravity	0.0676	m
\mathcal{K}_α	aerodynamic coefficient of thrust	3.68×10^{-5}	$\text{N/rad}^2\text{s}^2$
\mathcal{K}_β	aerodynamic coefficient of thrust	3.77×10^{-5}	$\text{N/rad}^2\text{s}^2$
γ_α	Aerodynamic coefficient yaw of upper rotor	1.47×10^{-6}	$\text{N.m.rad}^{-2}\text{s}^{-2}$
γ_β	Aerodynamic coefficient yaw of lower rotor	1.32×10^{-6}	$\text{N.m.rad}^{-2}\text{s}^{-2}$

2.3. Expression of linearized tangent model

The nonlinear system described by equation (2.16) will serve as a basis for the design of the control algorithms by nonlinear approaches, but it is absolutely not suitable for the synthesis of linear algorithms. However, these approaches are based on a dynamic model linearized around a certain point of operation, in this case hovering. The linearization assumptions of the nonlinear model relating to the hover are as follows:

- The translation speed v of the vehicle is small: $v = o(e)$,
- The position ξ of the vehicle is any,
- The rotation speed Ω of the vehicle is low $\Omega = o(e)$,
- Roll angle ϕ and pitch angle θ are low $\phi = \theta = o(e)$,
- The yaw angle ψ is regulated to zero.

The linearized model tangent to the vicinity of the hover is composed of the following four SISO (Single Input - Single Output) channels:

- An altitude chain having its state $[z \ v_z]^T$:

$$\begin{bmatrix} \dot{z} \\ \dot{v}_z \end{bmatrix} = \begin{bmatrix} 0 & 1 \\ 0 & 0 \end{bmatrix} \begin{bmatrix} z \\ v_z \end{bmatrix} + \begin{bmatrix} 0 \\ 1/m \end{bmatrix} T_z$$

- A rolling chain having its state $[y \ v_y \ \phi \ p]^T$

$$\begin{bmatrix} \dot{y} \\ \dot{v}_y \\ \dot{\phi} \\ \dot{p} \end{bmatrix} = \begin{bmatrix} 0 & 1 & 0 & 0 \\ 0 & 0 & g & 0 \\ 0 & 0 & 0 & 1 \\ 0 & 0 & 0 & 0 \end{bmatrix} \begin{bmatrix} y \\ v_y \\ \phi \\ p \end{bmatrix} + \begin{bmatrix} 0 \\ 0 \\ 0 \\ \frac{1}{J_{xx}} \end{bmatrix} \tau_t$$

- A pitch chain having its state $[x \ v_x \ \theta \ q]^T$

$$\begin{bmatrix} \dot{x} \\ \dot{v}_x \\ \dot{\theta} \\ \dot{q} \end{bmatrix} = \begin{bmatrix} 0 & 1 & 0 & 0 \\ 0 & 0 & -g & 0 \\ 0 & 0 & 0 & 1 \\ 0 & 0 & 0 & 0 \end{bmatrix} \begin{bmatrix} x \\ v_x \\ \theta \\ q \end{bmatrix} + \begin{bmatrix} 0 \\ 0 \\ 0 \\ \frac{1}{J_{yy}} \end{bmatrix} \tau_t$$

- A string of lace having as state $[\psi \ r]^T$:

$$\begin{bmatrix} \dot{\psi} \\ \dot{r} \end{bmatrix} = \begin{bmatrix} 0 & 1 \\ 0 & 0 \end{bmatrix} \begin{bmatrix} \psi \\ r \end{bmatrix} + \begin{bmatrix} 0 \\ \frac{1}{J_{zz}} \end{bmatrix} \tau_N$$

3. QFT CONTROLLER OF COAXIAL MICRO-HELICOPTER

Quantitative Feedback Theory is a robust control design technique that uses feedback to achieve responses that meet specified specifications despite structured plant uncertainty and plant disturbances [14, 15]. This technique has been applied to many classes of problems such as Single Input Single Output (SISO), Multiple Input Single Output (MISO) and Multiple Input Multiple Output (MIMO) for both continuous and discrete cases. For this research, a SISO system is assumed for control law design and sequential loop closures are utilized as with the pole placement controller. The QFT design methodology is quite transparent, allowing the designer to see the necessary trade-offs to achieve the closed-loop system specifications [16, 17]. The basic steps of the procedure as shown in Figure 5 are presented in the following sub-sections. They are: [18-20]

- Plant model (with uncertainty), Templates generation and nominal plant selection $P_o(j\omega)$.
- Specify acceptable tracking models, which the closed-loop response satisfies, $T_{R L} \leq T_R \leq T_{R U}$, and determine tracking bounds
- Determine disturbance rejection models, T_D , based on disturbance rejection specifications, and determine disturbance bounds
- Loop-shaping the controller $G(j\omega)$.
- Synthesize nominal loop transfer function, $L_O(j\omega)$
- Pre-filter synthesis $F(j\omega)$.
- Simulation and Design Validation.

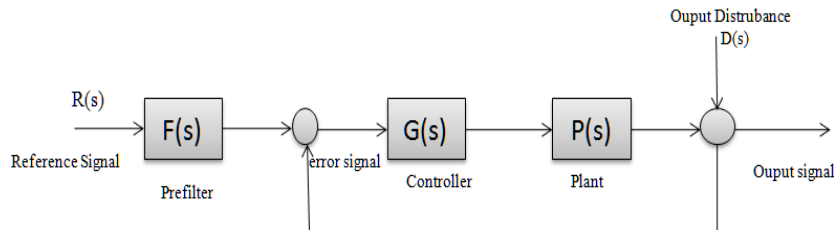


Figure 5. QFT control loop

3.1. Generating plant templates

Among the first step in Quantitative Feedback Theory (QFT) design process are generated the plant templates. The plant templates capture the uncertainties in the plant transfer function, $P(j\omega)$ and are plotted as boundaries of magnitude and phase variations on the Nichols chart at specific design frequencies. These templates are then used to create bounds on the Nichols chart as shown in Figure 5 [19, 21].

3.2. Generating performance bounds

Given the templates, QFT converts the closed loop magnitude specifications into magnitude and phase constraint on the open loop transfer function for the nominal plant ($L_0 = (G(s)P_0(S))$). Usually system performance is described as reference tracking, robust stability and rejection to input disturbance [20, 21].

- Reference Tracking

To meet the tracking performance the controller should satisfy to the following:

$$|T_l| \leq \left| F \frac{PG}{1+PG} \right| \leq |T_u| \quad (18)$$

where the upper T_u and lower T_l bounds are defined using time domain figure of merit such as peak overshoot and settling time.

$$T_u = \frac{(\omega_n^2/a)(s+a)}{s^2+2\varepsilon\omega_n s+\omega_n^2} / \omega_n = 1 \text{ rad/s}, \quad a=1, \varepsilon = 0.6 \quad (19)$$

$$T_u = \frac{s+1}{s^2+1.2s+1} \quad (20)$$

$$T_l = \frac{K}{(s+\sigma_1)(s+\sigma_2)(s+\sigma_3)} / \sigma_1 = 0.5, \sigma_2 = 1, \sigma_3 = 2, K = 1 \quad (21)$$

$$T_l = \frac{1}{(s+0.5)(s+1)(s+2)} \quad (22)$$

Numerical values ($\omega_n, a, \varepsilon, \sigma_1, \sigma_2, \sigma_3, K$) are taken from the specifications.

- Robust Stability

Robust stability in QFT amounts to checking stability using nominal plant ($L_0(s) = G(s)P_s(s)$) and then demonstrating stability of the whole set plants by assigning a sensitivity rating W_{s1} given by [19]:

$$\left| \frac{PG}{1+PG} \right| \leq W_{s1} = \mu \quad (23)$$

where:

μ is the circle M specification in magnitude:

$$M_m = 20 \log_{10}(\mu)$$

$$\Phi = 2 \cos^{-1}(0.5/\mu) \in [0, 180^\circ]$$

In [20], Oded Yaniv translated this condition to desired phase margin (PM) shown in (24) and gain margin (GM) shown in (25).

$$PM = 2 \sin^{-1}\left(\frac{1}{2(W_{s1})}\right), \quad PM \geq 180^\circ - \Phi \text{ (deg)} \quad (24)$$

$$GM = 20 \log\left(\frac{W_{s1}+1}{W_{s1}}\right), \quad GM \geq 1 + 1/\mu \text{ (magnitude)} \quad (25)$$

- Disturbance rejection at plant output

An upper limit is set to the sensitivity function to limit the peak value of disturbance amplification to the plant output as follow: [19-21]

$$\left| \frac{1}{1+PG} \right| \leq W_{dr} \quad (26)$$

$$W_{dr} = T_d = \frac{1}{1+PG} \leq \frac{s^2+2\varepsilon\omega_n s}{s^2+2\varepsilon\omega_n s+\omega_n^2} / \omega_n = 1 \text{ rad/s} \quad a=1, \varepsilon = 0.6 \quad (27)$$

$$T_d = \frac{1}{1+PG} \leq \frac{s^2+1.2s}{s^2+1.2s+1} \quad (28)$$

These bounds are then used for loop shaping to design a controller.

3.3. Controller design

The controller is designed by adding poles and zeroes to the nominal transfer function by satisfying all bounds at each frequency. During this stage, the designer considers a trade-off between the specification, controller complexity and the cost of feedback in the bandwidth [19-21].

$$G(s) = \frac{3.072(s-12)}{(s-350)(s-350)} \quad (29)$$

3.4. Pre-filter design

A pre-filter is needed to bring the response within the reference tracking tolerances, T_l and T_u and is done by adding poles and zeroes [19-21].

$$F(s) = \frac{1}{(s-0.30066)} \quad (30)$$

Simulation and validation of the design is shown in Figure 6 [22].

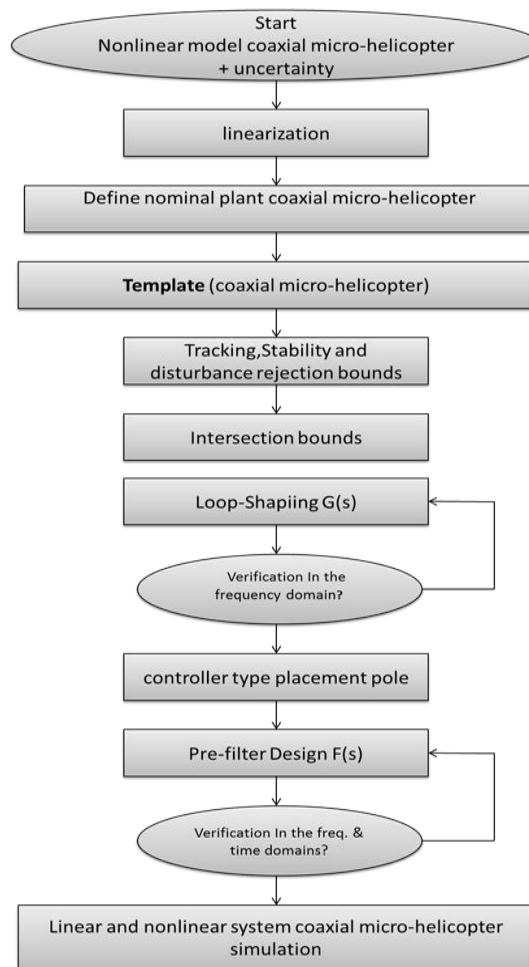


Figure 6. QFT design procedure

4. RESULTS AND ANALYSIS

The frequency range from 0.01 to 1000 rad/s was selected for the QFT controller design. This range covers the full range of frequencies for a typical coaxial micro-helicopter. The first step of the QFT design is to generate the plant templates. These plant templates were generated using the Matlab software [23] and are shown in Figure 7.

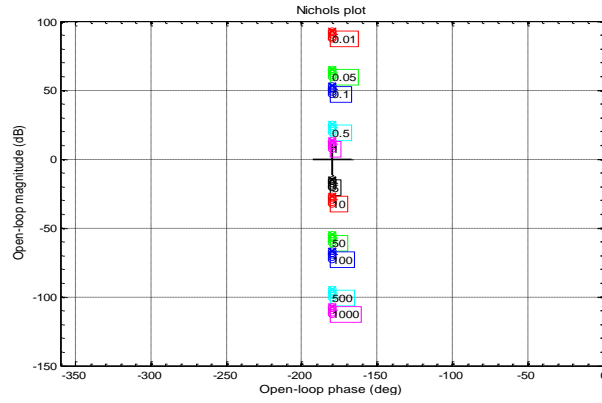


Figure 7. Plant templates

Criteria needed for the designing of the controller are:

- Tracking criterion

The upper bound for the tracking criterion was generated by considering 1.19% overshoot and settling time of 4.48 s. The transfer function used for the upper bound shown in (19). Similarly, the lower bound was generated by considering no overshoot and settling time of 9.77s. The transfer function used for the lower bound shown in (22). These bounds in time domain and frequency domain are shown in Figure 8. The tracking bounds are shown in the Nichols plot in Figure 9.

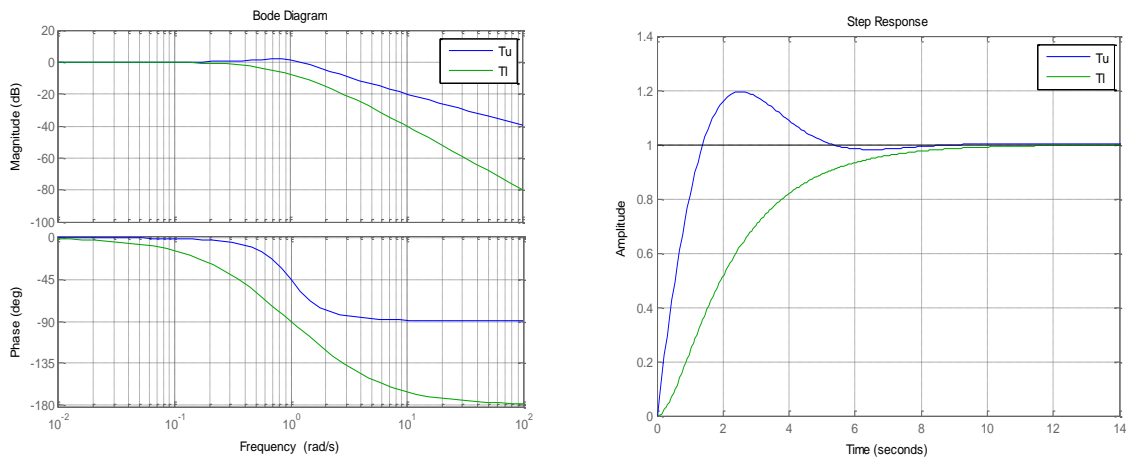


Figure 8. Tracking bounds; (a) time domain; (b) frequency domain

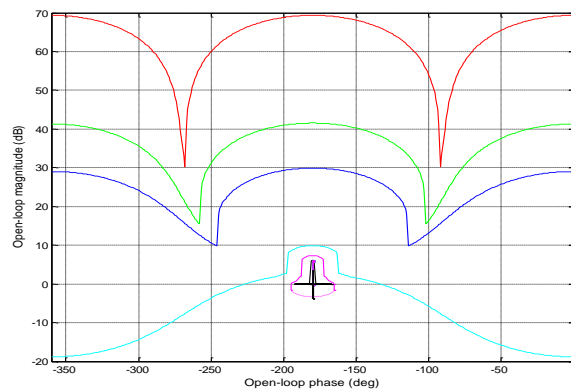


Figure 9. Intersection bounds (stability, tracking and disturbance rejection)

- Stability criterion

The sensitivity value W_s for the stability criterion is set to 1.1 which is translated to an allowable phase margin of 54° and a gain margin of 5.4 dB using (24) and (25). The stability bounds are generated on a Nichols plot and are shown in Figure 10.

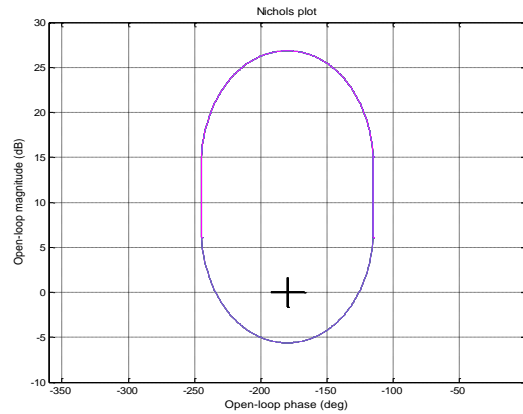


Figure 10. Stability bounds

- Disturbance rejection in the plant output

A performance criteria was set to reject disturbance in the output signal by setting the sensitivity value W_{dr} to 1.1. The resulting bounds are displayed in Figure 11.

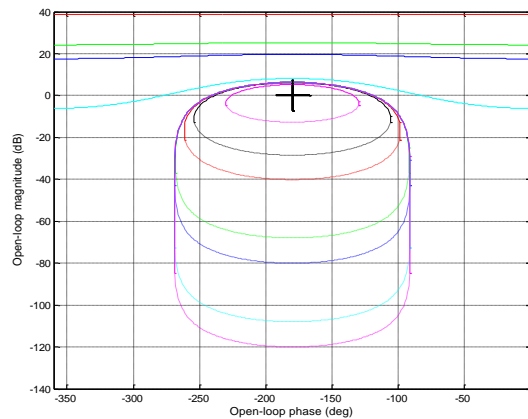


Figure 11. Disturbance rejection bounds

The stability bounds, tracking bounds and the disturbance bounds are combined into one Nichols plot. At each frequency the bound that has the highest gain are kept while the bounds with lower gains are rejected. These bounds as shown in Figure 12 and will be used to design the controller. The intersection bounds with nominal loop function without the controller are shown in Figure 13.

The nominal loop function shown in Figure 13 is the product of the nominal plant and the controller (to be designed). As seen, the points at each frequencies represented by the circles on the nominal loop are below the allowable gain and does not meet the specifications. The shape of the nominal loop function is changed by changing the gain of the controller and placing poles and zeros so that they meet the lowest possible gain required at each frequencies. Placing a real pole pushes the loop function to the left whereas adding a real zero pushes the loop function to the right. Increasing the gain of the controller increases the gain of the loop function there by moving the loop up on the Nichols plot. The transfer function controller designed to satisfy the performance criterion is shown in (29) and the tuned loop function is shown in Figure 14 [19, 21].

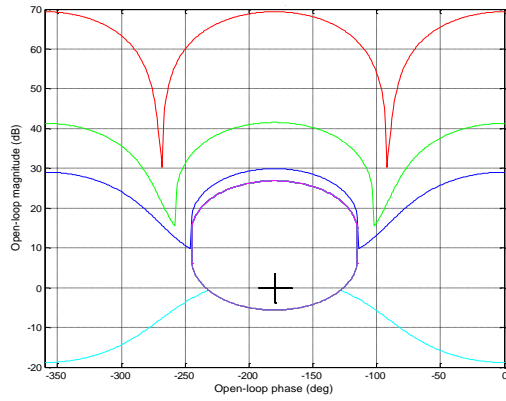


Figure 12. Intersection bounds

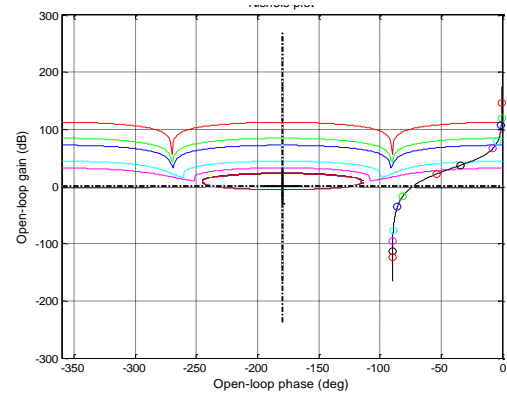


Figure 13. Nominal plant without controller

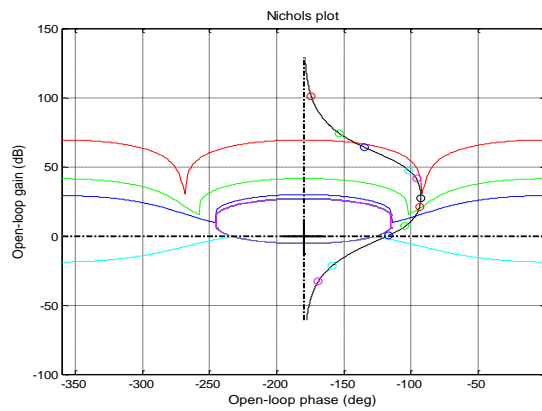


Figure 14. Tuned nominal plant (controller)

It can be seen that the nominal loop gain at each frequency is above the corresponding bound and is outside the stability bound, hence meeting all performance criteria. However, a prefilter has to be designed to meet the tracking criterion. Similar to the controller design, the prefilter is designed by placing poles and zeros to bring the response within the lower and upper bound of tracking criterion. Figure 15 shows the closed loop response of the plant with controller in frequency domain. It can be seen that the frequency response of the plant is above the upper bound limit.

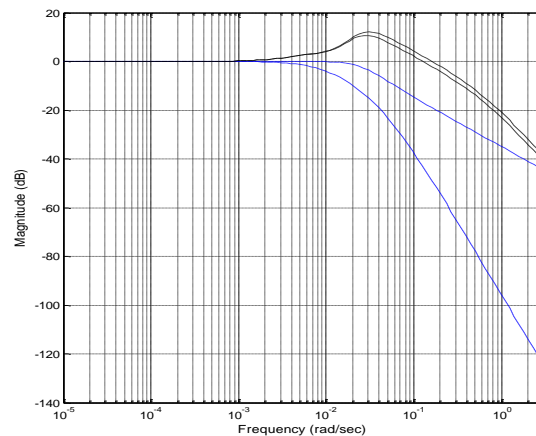


Figure 15. Plant response without prefilter

Hence, prefilter is needed to push the response below the upper bound limits. The prefilter designed to satisfy the tracking criterion is shown below and the plant response with prefilter is shown in Figure 16. Figure 17 illustrates the simulation results in the case of a time domain closed-loop for motion along the Z axis, and Figure 18 shows the unit step response for the disturbance rejection. The resulting simulation shows that the coaxial micro-helicopter is stable and meets tracking specifications.

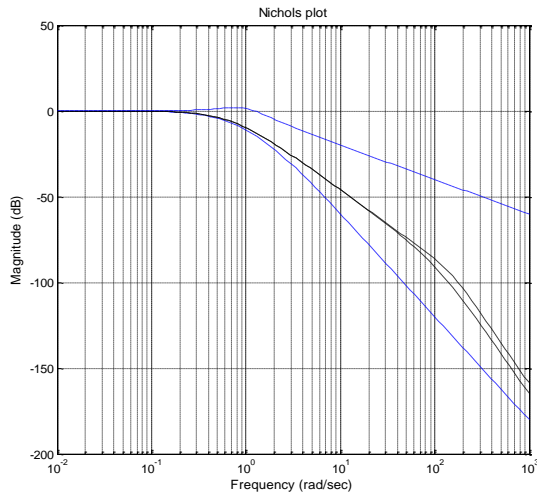


Figure 16. Plant response with prefilter

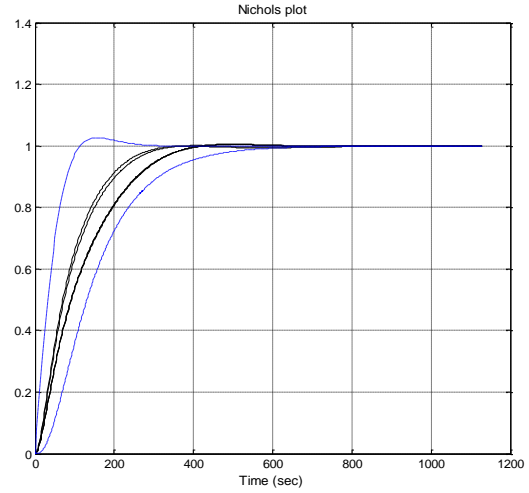


Figure 17. Unit step response (tracking); X axis: Time, Y axis: Altitude Z

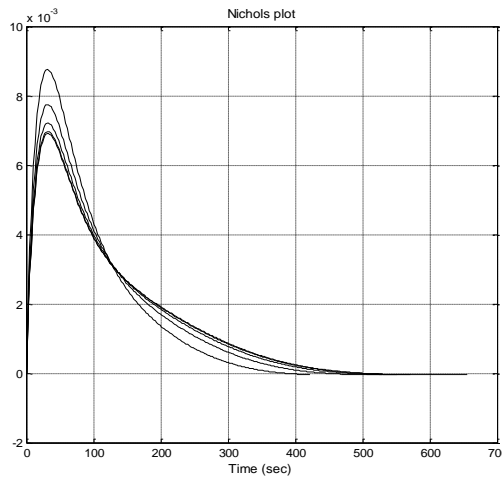


Figure 18. Unit step response (disturbance rejection) X axis: Time, Y axis: Altitude Z

The simulation results in the time domain closed-loop case for the Z-axis motion and the time response of the coaxial micro-helicopter roll, pitch, and yaw zero initial conditions were presented in Figure 19 and Figure 20. In order to compensate the uncertainties involved, a family of linear uncertain SISO systems is used. Then, pole placement-QFT as a robust controller maintaining zero steady state error, fast response (short rise time), lower oscillation and higher stability is selected. One of the main advantages of the pole placement controller robust controller is that it can be applied to higher order processes including more than single energy storage variables. A robust QFT controller for the linear process is designed for each SISO channel and nonlinear simulation in tracking step response indicates that the controller has consistence tracking ability, and disturbance rejection.

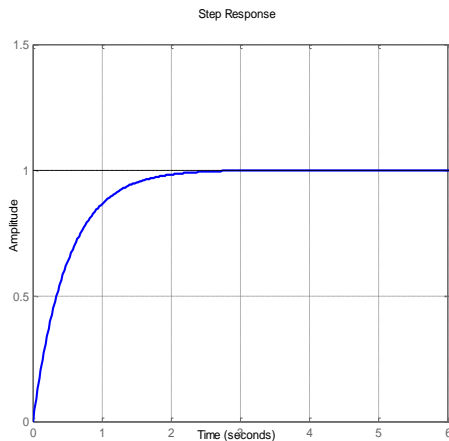


Figure 19. Nonlinear tracking response to control of altitude Z; X axis: Time, Y axis: Altitude Z

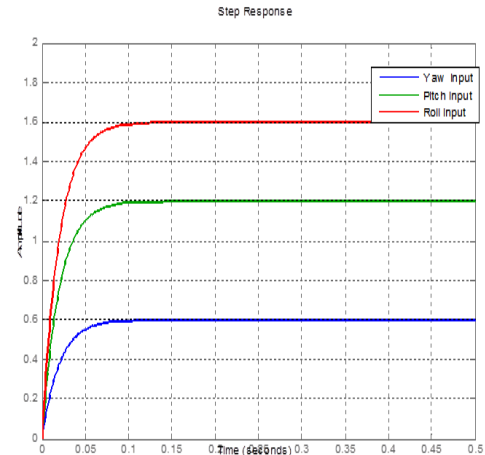


Figure 20. Nonlinear tracking response to control of angles X axis: Time, Y axis: Roll input=1, Pitch input=2, and Yaw input=3

5. CONCLUSION

In this paper, we presented a nonlinear model and a robust QFT control for the coaxial micro-helicopter. The use of Newton-Euler's formalism allowed us to establish the dynamic model of the coaxial micro-helicopter. From the model obtained, we conclude that the coaxial micro-helicopter is a nonlinear, mechanically complex system. Moreover, we can clearly see the complexity of the model, the non-linearity, the interaction between the states of the system. From certain hypotheses on the mechanical and aerodynamic model, it is possible to decouple the coaxial micro-helicopter model into four distinct chains (roll, pitch, yaw and altitude). This answers the problem of constructing the synthesis model for a quasi-stationary flight. Since the system is uncertain and noisy, we introduced a robust QFT command after linearization of the model. This frequency approach makes it possible to take into account the uncertainty of the process by frequency domain uncertainties called templates and built for a set of frequencies on the Black-Nichols diagram.

Instead of solving the synthesis problem for all possible states of the process, the QFT approach is based on controller synthesis for an arbitrarily chosen nominal system, while satisfying all the specifications for all processes. For this, the initial time of these specifications is first translated into frequency specifications. By taking uncertainty templates into account, these specifications are then translated into graphic constraints. Plotted on the Black-Nichols diagram, these constraints define the boundaries delimiting the different areas where the nominal open-loop frequency response must be localized for different frequencies. A regulator is first used to model the location of the Black-Nichols open loop and thus meet the part of the specifications pertaining to the rejection of disturbances and the uncertainty in the tracking of the deposit. A pre-filter is then synthesized in order to respect the part of the specifications relating to the tracking dynamics of the deposit. The simulation result obtained after the application of the QFT command on the coaxial micro-helicopter we conclude that the command proposed is a robust command.

REFERENCES

- [1] M. H. Or-Rashid, et al., "Inflow Prediction and First Principles Modeling of a Coaxial Rotor Unmanned Aerial Vehicle in Forward Flight," *International journal of aeronautical and space sciences*, pp.1-19, Dec 2015.
- [2] L.Chen and P.J.McKerrow, "Modeling the Lama Coaxial Helicopter," *Proceedings of the Australasian Conference on Robotics and Automation, Brisbane*, pp.1-9, 2007.
- [3] A. V. Clara and S.Redkar, "Dynamics and Control of a Stop Rotor Unmanned Aerial Vehicle," *International Journal of Electrical and Computer Engineering (IJECE)*, vol. 2, pp.1-12, Oct 2012.
- [4] D.Schafroth, et al., "Modeling and System Identification of the muFly Micro Helicopter," *Journal of Intelligent & Robotic Systems - Springer*, pp.27-47, Oct 2009.
- [5] A.Koehl, et al., "Modeling and identification of a launched micro air vehicle: Design and experimental results," *AIAA Modeling and Simulation Technologies Conference and Exhibit, Canada*, pp.1-18, Aug 2010.
- [6] A.Drouot, et al., "An Approximate Backstepping Based Trajectory Tracking Control of a Gun Launched Micro Aerial Vehicle in Crosswind," *Journal of Intelligent & Robotic Systems, Springer*, pp.133-150, Aug2012.

- [7] A.Nemati and M. Kumar, 'Control of Microcoaxial Helicopter Based on a Reduced-Order Observer,' *Article in Journal of Aerospace Engineering*, pp.1-8, Oct 2015.
- [8] Horowitz I.M., "Synthesis of feedback systems," Academic Press, New York, 1963.
- [9] Horowitz I.M., "Quantitative feedback design theory (QFT)," *IEEE Control Systems*, 1992.
- [10] R. Abbas and Q. Wu, "Improved Leader Follower Formation Control for Multiple Quadrotors Based AFSA," *TELKOMNIKA (Telecommunication Computing Electronics and Control)*, vol.13, pp. 85-92, Mar 2015.
- [11] M. R.Rahimi, et al., "Designing and Simulation for Vertical Moving Control of UAV System using PID, LQR and Fuzzy logic," *International Journal of Electrical and Computer Engineering (IJECE)*, vol. 3, pp. 651-659, 2013.
- [12] N. M. Raharja, et al., "Hovering Control of Quadrotor Based on Fuzzy Logic," *International Journal of Power Electronics and Drive System (IJPEDS)*, vol. 8, pp. 492-504, Mar 2017.
- [13] A. Al, et al., "An angle speed and thrust relationship of the quadcopter rotor," *Indonesian Journal of Electrical Engineering and Computer Science*, vol.13, pp.469-474, Feb 2019.
- [14] Horowitz I.M., "Survey of Quantitative Feedback Theory (QFT)," *International Journal of Robust and Nonlinear Control*, pp.887-921, Aug 2001.
- [15] Houpis C.H., et al., "Quantitative Feedback theory technique and applications," *International Journal of Control*, Taylor & Francis, pp.39-70, 1992.
- [16] Yaniv O., "Quantitative feedback design of linear and nonlinear control systems," *International Series in Engineering and Computer Science*, Springer, pp.1-367, 1999.
- [17] Houpis C. H., et al., "Quantitative Feedback Theory Fundamentals and Applications," Second edition, CRC Press, Taylor & Francis Group, 2006.
- [18] Moghadam A., et al., "Modeling and control of a SCARA robot using quantitative feedback theory," *Proc IMechE Part I. J SystContrEng*, pp. 901-918, Jun 2009.
- [19] M. R.Gharib and M.Moavenian, "Full dynamics and control of a quadrotor using quantitative feedback theory," *International journal of numerical modeling: Electronic networks, devices and fields*, pp.501-519, Aug 2015.
- [20] X. Xing and D. Yuan, "Quantitative Feedback Theory and Its Application in UAV's Flight Control," *Automatic Flight Control Systems*, pp.1-36, Jan 2012.
- [21] T. Wagner and J.Valasek, "Digital Autoland Control Laws Using Quantitative Feedback Theory and Direct Digital Design," *Journal of guidance, control, and dynamics*, pp. 1399-1413, Oct 2007.
- [22] M. G. Sanz, "Quantitative Robust Control Engineering: Theory and Applications," *In Achieving Successful Robust Integrated Control System Designs for 21st Century Military Applications*, pp.1-44, Sep 2006.
- [23] C.Borghesani, et al., "The QFT Frequency Domain Control Design Toolbox User's Guide," *Terasoft international Inc*, 2003.

BIOGRAPHIES OF AUTHORS



Aissa Meksi: Was born on 1981 in Mascara, Algeria. He received his B.S (State engineer) Engineering degree in automatism from University of Sciences and Technology of Oran (USTO), Algeria, in 2008. He received his M.S (Magister) degree in Electrical engineering specialty automatism from the same University in 2013. Currently, he is a PHD student at the same university. He is a member of LDEE Laboratory. He has published papers in various International Conferences. His research interests include the automated crane, unmanned aerial vehicle modeling, synthesis of a state observer of a uav, Control design of a Unmanned aerial vehicle.



Ahmed Hamida Boudinar received his PhD in University of Sciences and Technology of Oran Electrical Engineering Faculty. Department of Electrotechnics, Algeria. He is currently working as an Associate Professor in the Electrical Engineering Faculty at the University of Sciences and Technology of Oran BP 1505 AlMnaouar, 31000 Oran, ALGERIA. His research and teaching interests include: Maintenance and Diagnosis of Electrical Machines



Benatman Kouadri was born on 1950 in Saïda, Algeria. He received the B.Sc. degree in mechanical engineering from the Ecole Centrale de Nantes, Nantes, France, the M.Sc. degree and the Docteur-Ingénieur degree from the Faculty of Sciences, University of Nantes, and the Ph.D. degree in electrical engineering from University of Sciences and Technology of Oran, Oran, Algeria in 1978, 1982, 1985 and 2008, respectively. He is currently Full Professor at the University of Sciences and Technology of Oran (U.S.T.O.). Since 1975, he has published more than 30 papers in scientific journals and conference proceedings. He has also coauthored a book on power systems stability (in french). His main research interests include the simulation and modeling of Power Systems, FACTS Systems, Control of Dynamic Systems and the study of Electromagnetic Compatibility in Power Electronics circuits. His recent research interests have been focused on condition monitoring and fault detection of Induction Machines.